Thermal characterisation of rectangular cooling shapes in solids

Jaco Dirker
Department of Mechanical Engineering, Rand Afrikaans University, Johannesburg, South Africa, and
Arnaud G. Malan and Josua P. Meyer
Department of Mechanical and Aeronautical Engineering, University of Pretoria, South Africa

Received 7 June 2005
Revised 5 June 2006
Accepted 12 June 2006

Abstract

Purpose – This paper aims to investigate thermal geometric optimisation of rectangular heat conductive cooling structures within solid heat-generating media for the purpose of minimising peak temperatures and enabling optimum use of spatial volume within integrated power electronics.

Design/methodology/approach – A vortex-centred finite volume numerical solver was developed, employing a fully implicit solution algorithm to obtain 3D temperature distributions. By comparing the peak temperatures obtained for a wide range of related cases, optimised cross-sectional shapes for particular input conditions were obtained.

Findings – Optimum shapes are dependent on seven identified parameters. In cases where a low percentage of volume is occupied by cooling structures, a high tendency exists for continuous thin cooling layers, as opposed to discrete rectangular cooling inserts, to present the best thermal behaviour. At higher volume percentages, the opposite is true.

Practical implications – The reduced dimensions of cooling inserts have caused manufacturability to be a concern. Research has shown that at small dimensional scale ranges the cross-sectional shape of the cooling insert has little influence on its thermal performance. In such cases little or no thermal advantage or loss is incurred by making use of continuous cooling layers, which are easiest to manufacture.

Originality/value – The tendencies of optimum cooling structure shapes were obtained and described in terms of seven geometric and material property-related parameters. Thermal performance of individual inserts is not linearly proportional to dimensional scaling and it was found that, at small-scale ranges, optimisation from a manufacturing viewpoint would not significantly impact on thermal performance.

Keywords Thermal testing, Heat conduction, Cooling, Solids

Paper type Research paper

Nomenclature

A = x-y view cross-sectional area (m^2)
a = x-y view aspect ratio (dimensionless)
$a_{C,\mathrm{rel}}$ = relative x-y view aspect ratio of cooling insert (dimensionless)
C = heat equation coefficient
$\bar{C}_G$ = vector of heat gain coefficients
k = thermal conductivity (W/mK)
$\mathbf{M}$ = matrix of heat equation coefficients
M_2 = number of nodes in the x direction (dimensionless)
N_2 = number of nodes in the y direction (dimensionless)

International Journal of Numerical Methods for Heat & Fluid Flow
Vol. 17 No. 4, 2007
pp. 361-383

0961-5539
DOI 10.1108/09615530710739158

$\dot{q}''_C$ = heat flux at exposed face of cooling insert (W/m^2)
$\dot{q}'''_M$ = volumetric heat generation density (W/m^3)
R = thermal interface contact resistance (m^{2}K/W)
T = temperature (K or °C)
$\bar{T}$ = temperature vector (K or °C)
X = x directional distance between nodes shown in Figure 4
x = Cartesian coordinate, or distance between two neighbouring nodes in the x direction
Y = y directional distance between nodes shown in Figure 4
y = Cartesian coordinate or distance between two neighbouring nodes in the y direction
z = Cartesian coordinate

Greek and special symbols
α = fraction of volume occupied by cooling inserts (dimensionless)
γ = thermal conductivity ratio (dimensionless)
$\mathscr{A}$ = half centre-to-centre x-directional offset of neighbouring cooling inserts (m)
$\mathfrak{a}$ = half x-directional dimension of cooling insert (m)
$\mathscr{B}$ = half centre-to-centre x-directional offset of neighbouring cooling inserts (m)
$\mathfrak{b}$ = half y-directional dimension of cooling insert (m)
$\mathscr{L}$ = half z-directional dimension of structure (m)

Subscripts
B = relative rear direction (negative z direction)
C = cooling insert
D = whole domain
E = relative easterly direction (positive x direction)
F = relative frontal direction (positive z direction)
G = heat gain or heat loss
M = heat-generating medium
max = maximum
min = minimum
N = relative northerly direction (positive y direction)
S = relative southerly direction (negative y direction)
T = relative current node indication
W = relative westerly direction (negative x direction)
0 = reference cooling insert temperature

Introduction

The current trend in power electronics is to increase the power conversion capability of circuits while reducing their size (Ferreira and Gerber, 2002; Wolfgang *et al.*, 2002). An emerging method of doing this involves the 3D integration of discrete components into multifunctional modules and the creation of standardised building blocks (Liu and Lu, 2000; Van Wyk *et al.*, 2002; Lee *et al.*, 2002; Yang *et al.*, 2003). This can be done by using planar type structures or modules with various layers (Barbosa *et al.*, 2002).

In order to satisfy future thermal demands associated with, for instance, integrated power electronic devices, the focus is starting to shift toward innovative design of the internal structure of power modules to assist in heat extraction while maintaining high levels of electromagnetic performance and efficiency. Such an integrated power electronics system requires advances in different technologies, which depend upon finding solutions to deal with the multidisciplinary issues in materials, electromagneti-c compatibility and thermal management.

New types of integrated power electronic modules are usually proposed with a layered type of configuration (Strydom and Van Wyk, 2002). Therefore, the cooling inserts would need to have rectangular cross-sections rather than rounded ones, which would not be as easy to accommodate within other rectangular type regions. By characterising the effect of various parameters on the optimum shape in such cooling structures, the design of the embedded cooling systems may be effectively conducted in terms of thermal conductivities of materials involved, dimensions under consideration, thermal interface resistances between heat-generating and cooling materials, etc.

It is the aim of this paper to describe the optimum aspect ratio of a cooling insert's cross-section to minimise the peak temperature within the heat-generating medium. For this purpose, a problem-specific numeric code has been developed and a numerical investigation performed to determine and characterise the influence of various geometric and thermally related parameters on the optimum shape. No reference material was found in the literature to adequately document this.

Model problem

Consider Figure 1, which shows a representation of the proposed cooling insert layout. The aim of the latter is to effect heat flow from within a heat-generating medium to a device placed on the outside of the electronic component, such as a heat sink. The sectioned view shows a generalised distribution of evenly spaced identical rectangular heat extraction inserts that are aligned with the *z* Cartesian coordinate axis. Arrows indicate the direction of heat flow from the heat-generating medium via the heat extraction inserts. The model problem involves two materials from a heat conduction point of view, namely the heat-generating material and the cooling insert.

It is typical that the characteristic dimensions of the above grid-like structure (e.g. cooling insert dimensions and spacing) are small in comparison with the actual electronic component, and that the grid is thermally isolated from the ambient at its boundary faces, other than those parallel to the *x-y* plane. It may further be expected that each heat extraction structure will be exposed to an isothermal uniform ambient in an identical way. This implies that the rectangular regions drawn around each cooling structure (such as those in Figure 1 indicated by dotted lines) would have identical temperature distributions.

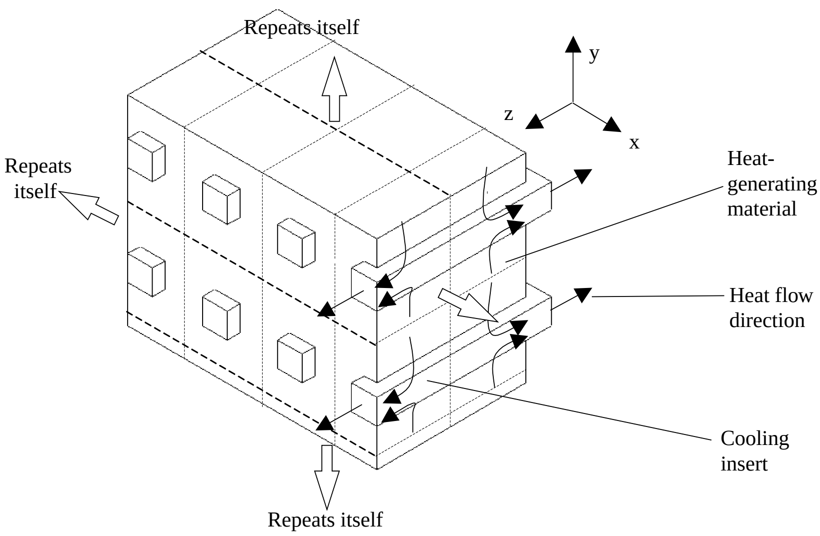

Figure 1.
Representation of a typical section of a heat-generating material with embedded cooling structures

For the above, symmetry in the heat-conduction phenomenon is such that the problem may be reduced to the representative section shown in Figure 2. Note that the heat extraction insert is exposed to the surroundings on its positive z side face. Here, z (m) denotes the half-length of the heat-generating material, which was defined in order to determine what influence the component length has on both temperature distributions and optimum cooling insert geometric tendencies.

The partial differential governing equation that describes the temperature at each point within the cooling structure, as well as within the heat-generating section of the model, can be expressed as follows:

$$\frac{\partial}{\partial x}\left(k\frac{\partial T}{\partial x}\right)+\frac{\partial}{\partial y}\left(k\frac{\partial T}{\partial y}\right)+\frac{\partial}{\partial z}\left(k\frac{\partial T}{\partial z}\right)+\dot{q}'''=0 \tag{1}$$

Note that the above equation does not hold at the bi-material interface. For this, an interface resistance is employed. At the interface, the temperature is seen as a discontinuity in equation (1) governed by the following equation:

$$\Delta T = q''R \tag{2}$$

Here, ΔT is the temperature difference across the interface, q'' (W/m^2) refers to the heat flux over the interface and R (m^{2}K/W) is the thermal interfacial resistance.

The temperature difference. Boundaries were defined as being adiabatic, except for the positive z side face of the heat extraction insert where a uniform heat flux $\dot{q}''_C$ (W/m^2) was defined to the surroundings so that all heat generated within the volume would be extracted to the ambient. This is valid if it is assumed that, during cooling, the majority of heat removal occurs via conduction (this is expected to be the case if cooling inserts are appropriately designed). The resulting heat flux can be calculated in

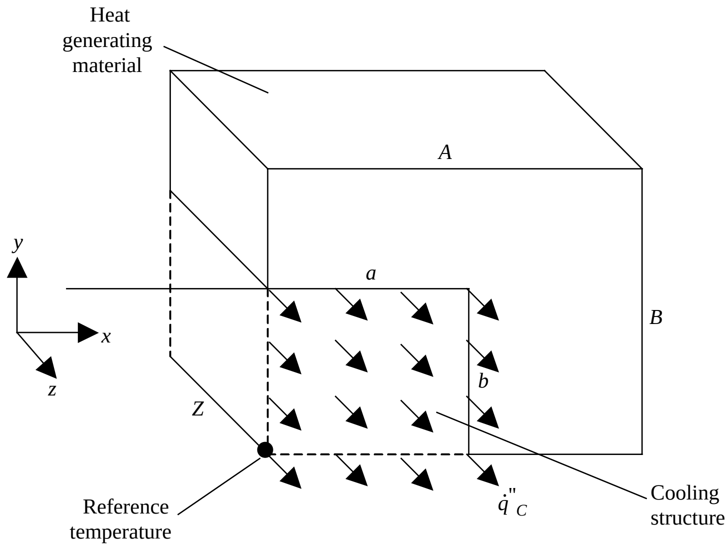

Figure 2.
Schematic view of the representative bi-material model problem

terms of the model problem dimensions, as well as in terms of the volumetric heat generation density, $\dot{q}'''_M$(W/m^3), within the representative domain as follows:

$$\dot{q}''_C = -\frac{\dot{q}'''_M(\mathscr{A}\mathscr{B} - \mathfrak{a}\mathfrak{b})\mathscr{Z}}{\mathfrak{a}\mathfrak{b}} \tag{3}$$

Here, $\mathscr{A}$, $\mathfrak{a}$, $\mathscr{B}$, $\mathfrak{b}$ and $\mathscr{Z}$ are the dimensions of the representative domain as shown in Figure 2.

The temperature at $x = 0, y = 0$ was prescribed (Dirichlet boundary condition) to be $T_C = 0$ in order to fix the reference temperature during the solution process. The arbitrary choice of T_C is valid since absolute temperatures are not of interest in this investigation. What is pivotal, however, is the peak relative temperature (temperature increase).

Problem reduction: characteristic relation variable definition

In order to simplify the intended thermal characterisation study, different relations and parameters were defined. Especially, the symmetric geometry of the model problem lends itself to the definition of a number of spatial dimension relations. Four of these are described below.

The aspect ratios in the *xy*-plane of the overall domain and the cooling structure were defined, respectively, as follows:

$$a_D = \frac{\mathscr{A}}{\mathscr{B}} \geq 1 \tag{4}$$

$$a_C = \frac{\mathfrak{a}}{\mathfrak{b}} \tag{5}$$

Note that only $a_D \geq 1$ was investigated, as the mirror behaviour for is $a_D \leq 1$ equivalent. For instance, $a_D = 2$ would give the same results as $a_D = 0.5$ by merely rotating the x and y axes through 90°.

Next, the cross-sectional area of the entire representative domain in the *xy* view and the volumetric fraction occupied by the cooling structure, α, can be expressed, respectively, as:

$$A_D = \mathscr{A}\mathscr{B} \tag{6}$$

$$\alpha = \frac{A_C}{A_D} = \frac{\mathfrak{a}\mathfrak{b}}{\mathscr{A}\mathscr{B}} \tag{7}$$

Here, A_C (m^2) represents the *xy* view cross-sectional area of the model problem.

In conjunction with the depth z, the four variables namely A_D (m^2), a_D (dimensionless), a_C (dimensionless) and α (dimensionless) fully define the problem in geometric terms.

The geometric constraints on the relative size of the cooling inserts lead to the definitions of the following maximum and minimum values of the cooling insert aspect ratio, a_C:

$$a_{C,\min} = \alpha a_D \tag{8}$$

$$a_{C,\max} = \frac{a_D}{\alpha} \tag{9}$$

The material property-related non-dimensional relation employed in this study is the ratio between the thermal conductivity of the cooling structure k_C (W/mK) and thermal conductivity of the heat-generating material k_M (W/mK) as:

$$\gamma = \frac{k_C}{k_M} \tag{10}$$

This proved to be of value in investigating the influence of material thermal conductivities within the model problem on the temperature distribution.

Thermal interface resistance between the heat-generating and cooling materials was defined to be uniform and was represented in the study by R (m^2K/W).

Numerical method

Finding an analytical solution to the bi-material problem shown in Figure 2 proved to be elusive. Since, performing an experimental geometric shape optimisation would also have been prohibitively time consuming, a numerical approach was employed for the purpose of this investigation.

In order to use a numerical solution method, the domain was decomposed into hexahedral elements defined around nodal points. Owing to the rectangular nature of the model problem, the use of such a type of element was convenient. A schematic representation of the distribution employed for a nodal point is shown in Figure 3. The number of nodes shown here is not necessarily the number used during simulations. An important point to note is that no nodes were defined on the interface between the cooling structure and the heat-generating medium. When nodes were defined on boundaries it resulted in non-physical discontinuities in the predicted temperature solutions. This was most evident when thermal contact resistance at the interface was defined to be small or absent.

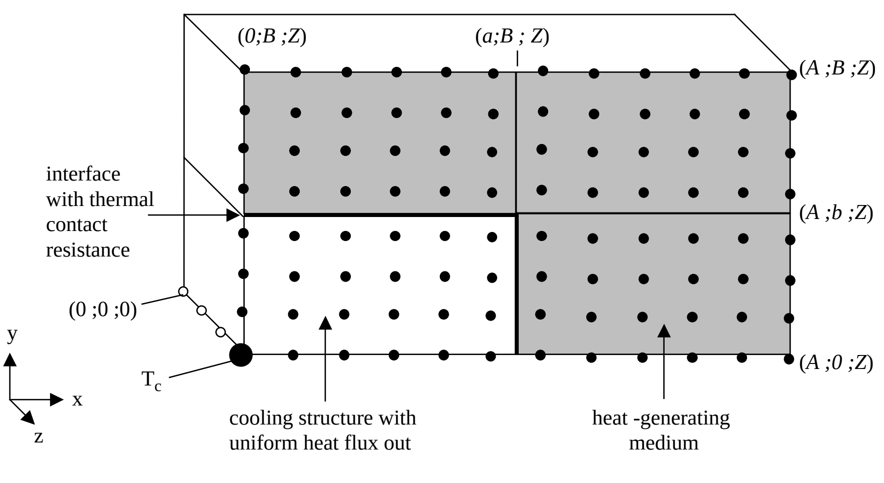

Figure 3.
Distribution of nodal points

The grid used was localised uniformly in such a way that each block shown in Figure 3 had uniform grid spacing. Although the entire mesh was not necessarily uniform in the x or y directions, uniform grid spacing was however used in the z direction.

Numerical simulation involves three separated stages, namely pre-processing, processing or solution, and post-processing. Pre-processing includes the definition of domain dimensions, specification of thermal properties and boundary conditions, mesh creation, and solution method specification. Owing to the large number of anticipated simulation cases that would be needed to optimise cooling structure shapes and distribution, the conventional pre-processing stage would become very protracted and tedious if commercially available numerical simulation software packages were to be used. For this reason the option was to create a computer code that would allow complete automation of the pre-processing stage for various combinations of problem geometry and thermal properties.

As a result of the relatively simple boundary condition and structured grid scheme required by the model problem, the more traditional vortex-centred finite volume numerical method was employed. With this method, the governing differential equation is discretised for rectangular 3D control volumes and the variable being solved (in this case temperature) is expressed in terms of variable values of neighbouring control volumes by a single linear type equation.

For the above grid structure type used, the governing equation (1), can be discretised in such a way that the temperature at a particular node can be expressed in terms of the temperatures at neighbouring nodes (Patankar, 1980):

$$C_T T = C_F T_F + C_S T_S + C_W T_W + C_E T_E + C_N T_N + C_B T_B + C_G \tag{11}$$

Constant coefficients C_F, C_S, C_W, C_E, C_N, and C_B refer to the six reference directions, "front", "south", "west", "east", "north", and "back", respectively, as shown in Figure 4. The subscript T refers to the temperature node under consideration, and G indicates the heat gain or heat loss of the control volume about the particular node.

By way of example, the coefficients for a node located at a position with adiabatic boundaries to the positive z direction and negative y direction, are calculated as follows:

$$\left.\begin{array}{c} C_F = 0 \\ C_S = 0 \\ C_W = 2x_E y_N^2 z^2 \\ C_T = 2X\left[x_E x_W\left(y_N^2 + z^2\right) + y_N^2 z\right] \\ C_E = 2X x_E x_W z^2 \\ C_N = 2X x_E x_W z^2 \\ C_B = 2X x_E x_W y_N^2 \\ C_G = \frac{\dot{q}_M'''}{k_M} X x_E x_W y_N^2 z^2 \end{array}\right\} \tag{12}$$

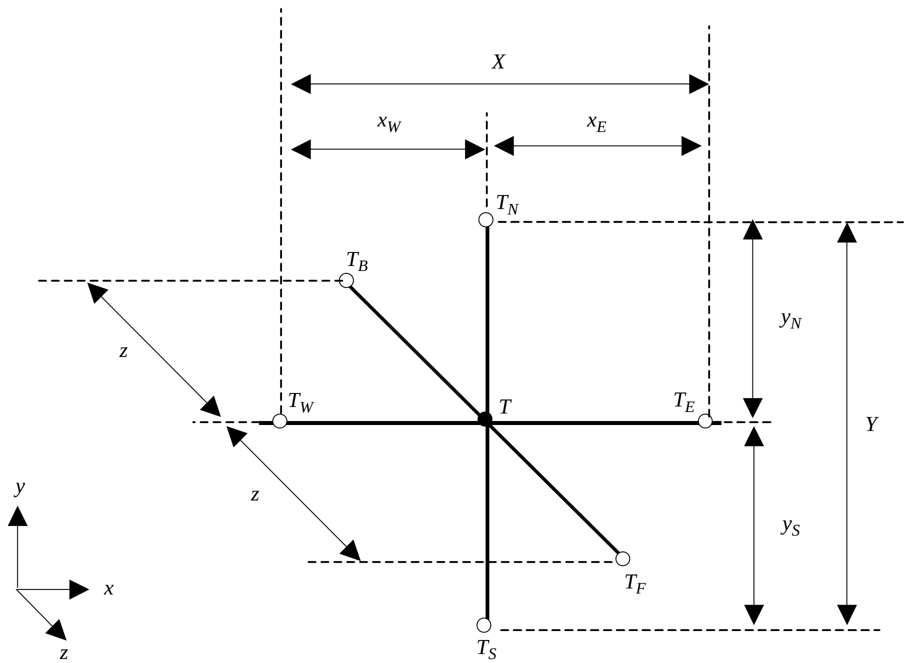

Figure 4.
Definition of reference directions and distance dimensions between neighbouring temperature nodes

If there are N nodes, N number of equations is required to solve the temperature values at all grid points. The resulting set of discrete equations can be expressed in matrix format as:

$$\mathbf{M}\bar{T} = \bar{C}_G \tag{13}$$

Here, $\mathbf{M}$ is an N-by-N coefficient matrix. The coefficient matrix is very sparsely populated with the majority of entries being zero. The conventional classic method of solving the temperature vector would be to use a Gauss-Jordan elimination to obtain the inverse of the matrix. However, its banded structure calls for a more efficient solution procedure. One such a method is LU-decomposition, whereby the banded coefficient matrix is subdivided into an upper and lower triangular matrix. From this, backward and forward substitution can be used to obtain the temperature solution. Note that, according to Fröberg (1985), only the banded part of the matrix features in the solution process, making for efficient inversion.

As the chosen solution method deals only with entries within the outer diagonals, the number of computations needed can be reduced further if the bandwidth of $\mathbf{M}$ is decreased. This can be done by using a bandwidth-reducing numbering scheme. The reverse Cuthill-McKee algorithm (Cerdán *et al.*, 2002; Gajewski and Lompies, 1999) was selected for this purpose.

The percentage reduction in the bandwidth resulting from the reverse Cuthill-McKee algorithm (compared with the structured numbering scheme) for three different size matrices with different numbers of nodes in the *z* direction is shown in Figure 5. It was found that for a structured 2D mesh, where there is only one node in the z direction, there is no reduction in the bandwidth of the matrix. As shown, it is most advantageous to apply the reverse Cuthill-McKee algorithm where the mesh has a width of two nodal points in the z direction.

Code validation

In cases where $k_C \rightarrow \infty$, and $\mathfrak{b} \rightarrow \mathscr{B}$ or $\mathfrak{a} \rightarrow \mathscr{A}$, the temperature field within the domain should approach a 1D type distribution. In case of $\mathfrak{b} \rightarrow \mathscr{B}$, this may be described by the following analytical equation:

$$T(x) = \dot{q}'''_M \left[\frac{(\mathfrak{a}^2 - x^2)}{2k_M} + \frac{\mathscr{A}(x - \mathfrak{a})}{k_M} + (\mathscr{A} - \mathfrak{a})R \right] + T_C \tag{14}$$

Note that due to the infinite thermal conductivity of the cooling insert (k_C), the applied reference temperature T_C, is propagated through the entire length of the cooling insert. The temperature distribution in the domain is consequently independent of z.

The numerical code developed here was tested by increasing k_M and allowing $\mathfrak{b}$ to approach $\mathscr{B}$. It was found that the numerically obtained solution approached the above analytical expression as $\mathfrak{b} \rightarrow \mathscr{B}$ for the example case shown in Figure 6. The mesh employed contained ten nodes in both the x and y directions. As shown in Figure 7, an excellent agreement was obtained between predicted and analytical solutions. This was found to be the case for the entire range of dimensional and thermal property values employed in this work.

Another method of validating the numerical code developed was to compare its results with that of a well-established commercial numerical software package. Fluent version 6.1.22 was used for this purpose to obtain mesh independent solutions. An arbitrary example case was set up, representing a condition where 25 per cent of the

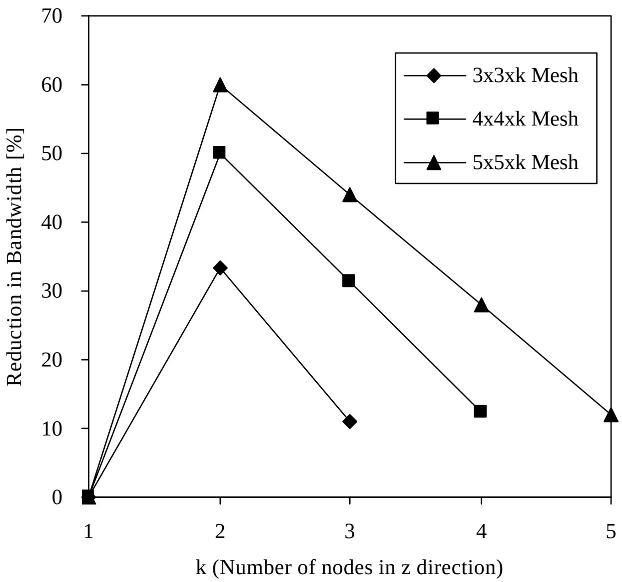

Figure 5.
Reduction in matrix bandwidth after applying the Reverse Cuthill-McKee algorithm

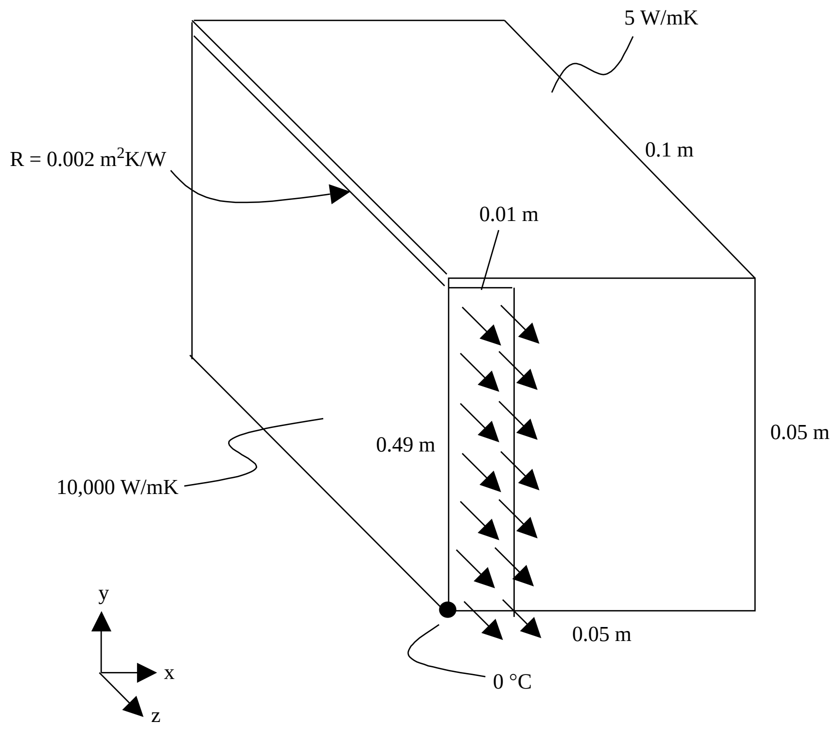

Figure 6.
Example case approximating a one-dimensional set-up

volume was occupied by arbitrary square cooling inserts spaced evenly in both the x and y directions. Figure 8 shows this schematically, as well as a representation of the meshes used. The temperature profiles obtained from the developed numerical code and fluent when $y = 0$ and $y = \mathscr{B}$ with $z = 0$ and $z = \mathscr{L}$, are shown in Figure 9. An excellent agreement was again obtained, which validated the accuracy of the developed code.

In the above validation study, mesh independence was found to prevail when ten or more nodes were used in the x, y, and z directions. Above ten nodes, the temperature distributions would differ by less than 1 per cent each time the number of nodes doubled. All subsequent simulations were conducted using ten nodes in each of the Cartesian coordinate directions.

Numerical optimisation study and results

By running a sequence of simulations, the optimum cooling structure shape can be found for a particular representative domain geometry and thermal condition.

Strategy

During initial analyses it was found that when $a_D \geq 1$, the optimum case with the lowest peak temperature is always associated with a cooling structure aspect ratio, a_C, in the range of $[a_D; a_{C,\max}]$. Here, the maximum value of a_C can be expressed as follows:

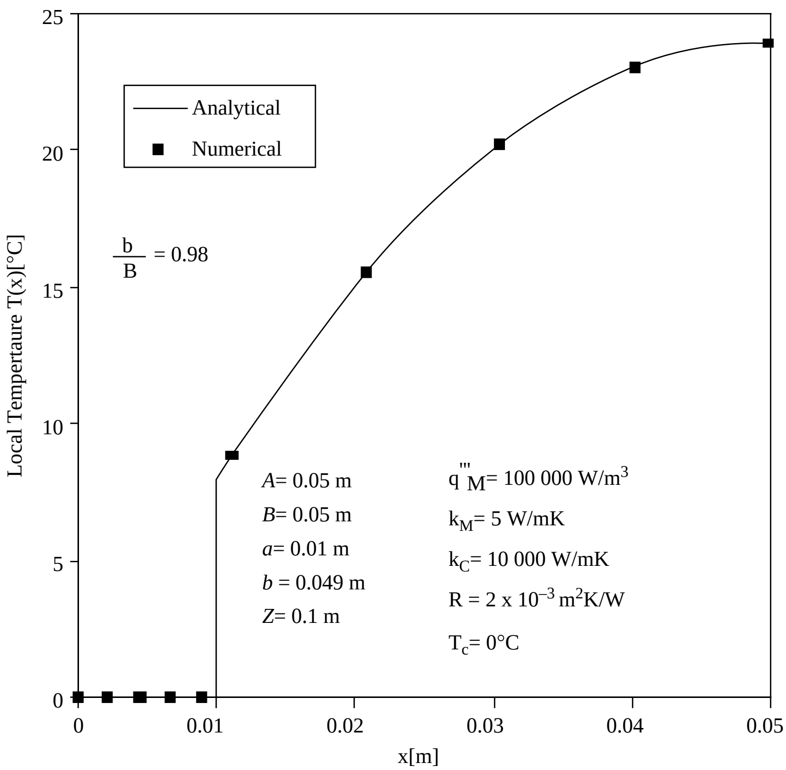

Figure 7.
Numerically obtained solution compared to the one-dimensional analytical profile (a) dimensions, (b) mesh used by fluent, (c) mesh used by numerical code

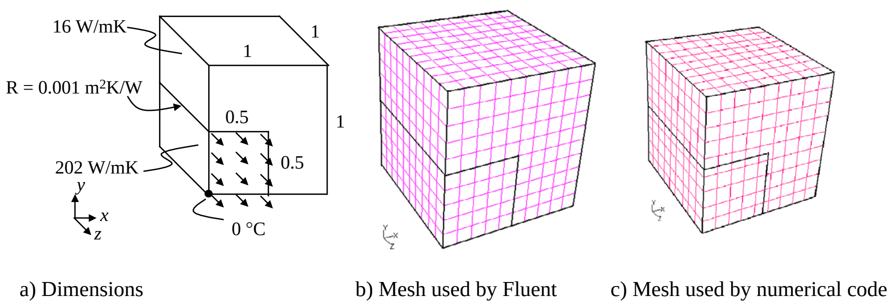

Figure 8.
Example case used for 3D verification

$$a_{C,\max} = \frac{a_D}{\alpha} \tag{15}$$

It is therefore convenient to normalise a_C with respect to this range by defining a new relative cooling aspect ratio, namely $a_{C,\mathrm{rel}}$:

$$a_{C,\mathrm{rel}} = \frac{a_C - a_D}{a_{C,\max} - a_D} \tag{16}$$

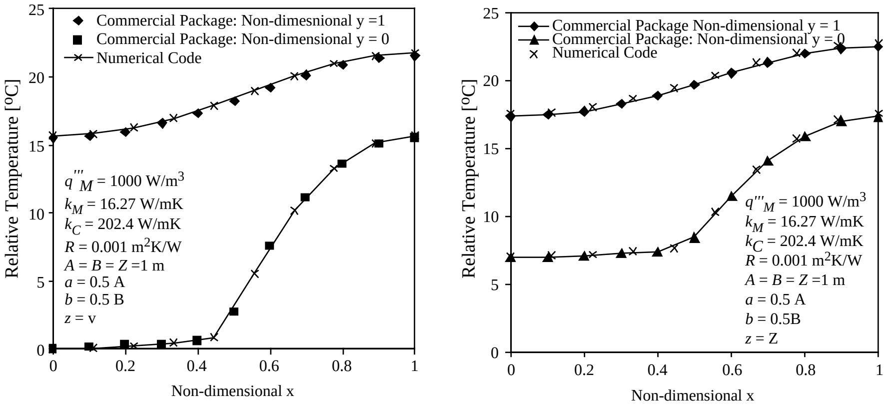

Figure 9.
Comparison between numerical code and commercial numerical software solutions at a) $z = 0$; b) $z = \mathscr{Z}$

When $a_{C,\text{rel}} = 1$, it means that the cooling insert is at its maximum aspect ratio as shown in Figure 10. When $a_{C,\text{rel}} = 0$, the cooling insert has the same aspect ratio as the representative problem domain.

Furthermore, initial runs showed that the maximum temperature in the domain ($T_{\max}$) is directly proportional to $\dot{q}_M'''$. Also, an increase or decrease in the cooling structure temperature, T_C, is translated directly into an identical increase or decrease in $T_{\max}$. This means that neither $\dot{q}_M'''$ nor T_C has any influence on the shape of the optimum cooling geometry. Mathematically this can be expressed as:

$$T_{\max} - T_C \propto \dot{q}_M''' \tag{17}$$

The influence of seven identified independent parameters on the optimum shape, namely, a_D, A_D, α, $\mathscr{Z}$, k_M, k_C and R was investigated and is documented below. This was done by performing a sequence of optimisation runs where only one of these parameters was altered during each sequence. Finally, by comparing the obtained optimum cooling shapes for different combinations of these parameters, the optimum cooling shape trends could be identified.

Optimum $a_{C,rel}$ *results for* $a_D = 1$

A domain with a square cross-sectional area is applicable (i.e. $a_D = 1$) to an arrangement where the centre-to-centre cooling structure spacing in both Cartesian directions is identical. Figure 10 shows that when there is no thermal contact resistance, the physical size of the cooling insert has little influence on its optimum shape. This can be deduced from the fact that the six values of A_D (representing physical size) ranging from 0.0001 to $1\,\text{m}^2$ result in the same optimum shapes. Similarly, in Figure 11, the same is shown to be true of the effect of the depth of the domain, $\mathscr{Z}$, where seven different depth values (0.001 to 1 m) resulted in the same optimum shape value profile. In cases where less than approximately 70 per cent of the domain was occupied by cooling, the optimum cooling insert shape was found to be a flat continuous "plate" as shown in Figure 12.

Finally, in the case of negligible thermal interface resistance, the ratio between the thermal conductivities, γ (relative thermal conductivity of the cooling insert in terms of the heat-generating material or k_C/k_M) was found to play an important role. For such

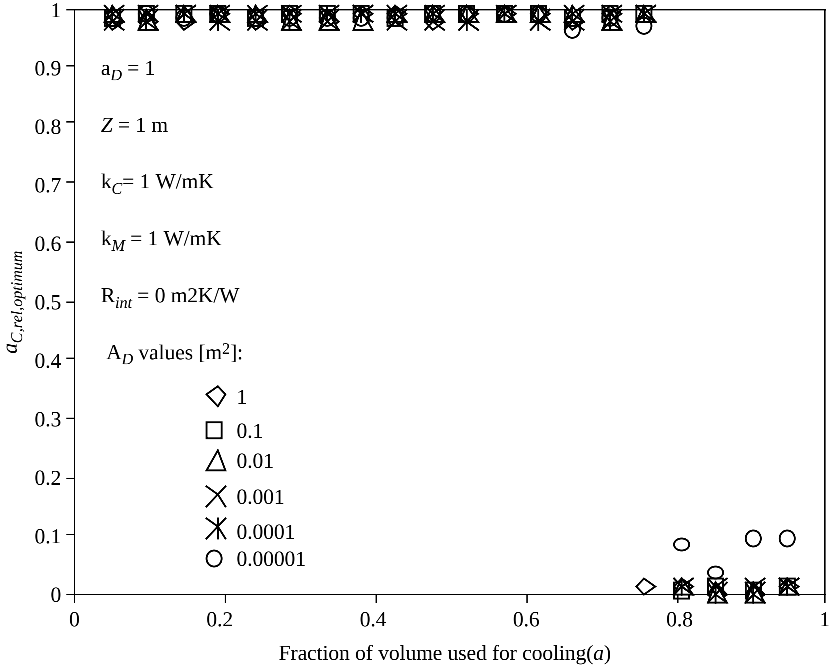

Figure 10.
The influence of the physical size of the cooling structures on the optimum cooling insert shape for a problem domain thickness of 1 m

conditions, scaling of the thermal conductivities exhibits the same optimisation results as long as the same ratio γ is maintained (Thus, when $k_M = 1\,\text{W/mK}$ and $k_C = 3\,\text{W/mK}$, it would result in the same optimum shapes as when $k_M = 2\,\text{W/mK}$ and $k_C = 6\,\text{W/mK}$). Figure 13 shows the calculated optimum cooling shapes for various γ ratios when no thermal interface resistance is present.

The case of non-zero thermal interface resistance is considered next. In Figures 14 and 15, the influence of R for different example values of A_D is plotted. From this it can be seen that even though the general trends are similar, different “peal off” lines for different R values are present as A_D is changed. By comparing Figure 15 with Figure 16, the influence of R for different $\mathscr{Z}$ values is demonstrated. Once again, a change in $\mathscr{Z}$ results in different optimum cooling shape lines as R is changed. Finally, as is shown in Figure 17, the scaling magnitude of the thermal conductivities, even while a constant γ is maintained, influences the optimum cooling aspect ratio when interface thermal resistance is present. As opposed to when there is zero thermal interface resistance, the magnitudes of thermal conductivities need to be taken into account when calculating optimum cooling shapes.

From Figures 14 through to 17, it can be observed that the presence of thermal interface resistance results in the relative optimum aspect ratio deviating from the $a_{C,\text{rel}} = 1$ line at an earlier α value than when thermal interface resistance is not present. In some cases, different R values have the same optimum $a_{C,\text{rel}}$ as shown in Figures 14 and 15.

Oscillations present at the cross-over points in some regions of the curves indicate a high level of sensitivity of the optimum shape in terms of the fraction of the volume

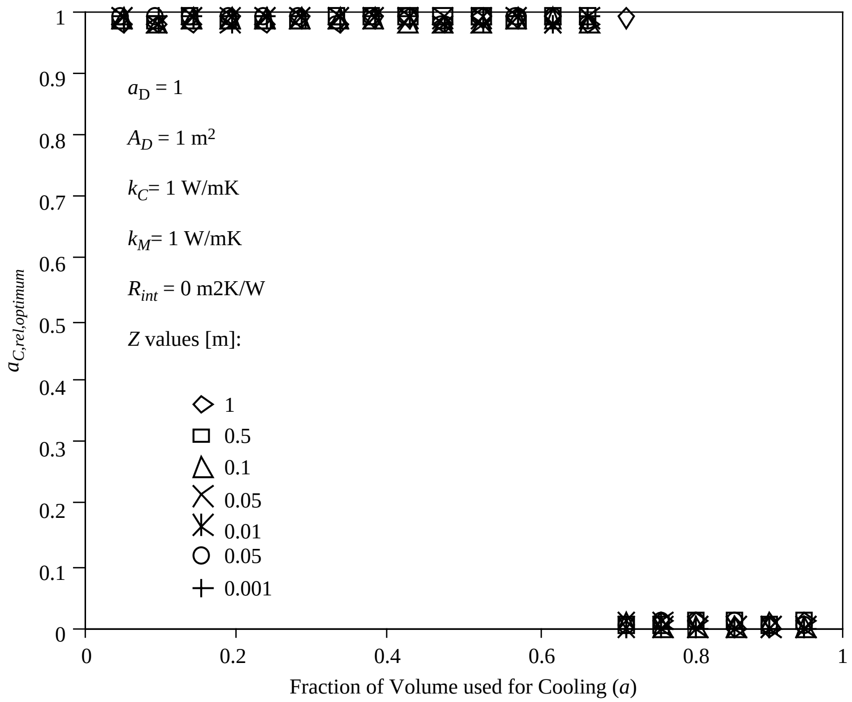

Figure 11.
The influence of the z direction depth on the optimum cooling insert shape for a domain area of 1 m^2

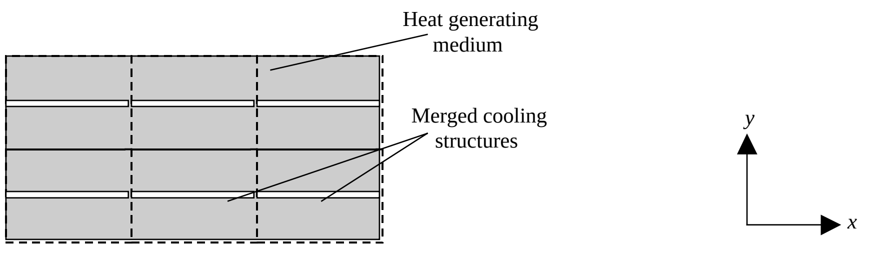

Figure 12.
Physical representation of the case where a_C is at its maximum

used for cooling (α). The oscillation seen in Figure 11 for one of the cases investigated is non-physical and is the result of the resolution of the numerical optimisation-searching algorithm. Owing to the fact that these oscillations are present in the region when more than 80 per cent of the volume is occupied by cooling layers, it can be disregarded due to practical reasons. Occupying such a large fraction for cooling purposes would be impractical.

Some lines in Figures 13-16, which do not appear to be smooth, are also due to the resolution of the optimisation algorithm. It was found that these slight variations (of less than 3 per cent) disappear when increasing the searching resolution. The slight increase in accuracy which can be obtained by doing so could however not be warranted when considering the dramatic increase in computational cost involved.

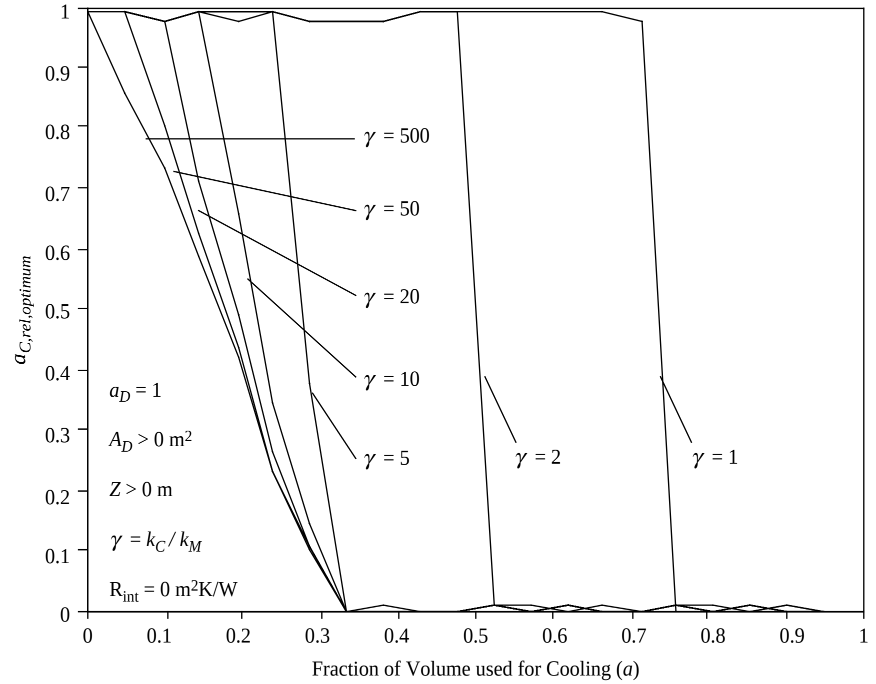

Figure 13.
Influence of γ on $a_{C,\text{rel,optimum}}$ for $A_D = 1\,\text{m}^2$, $\mathscr{Z} = 0.001\,\text{m}$, and $R = 0\,\text{m}^2\text{K/W}$

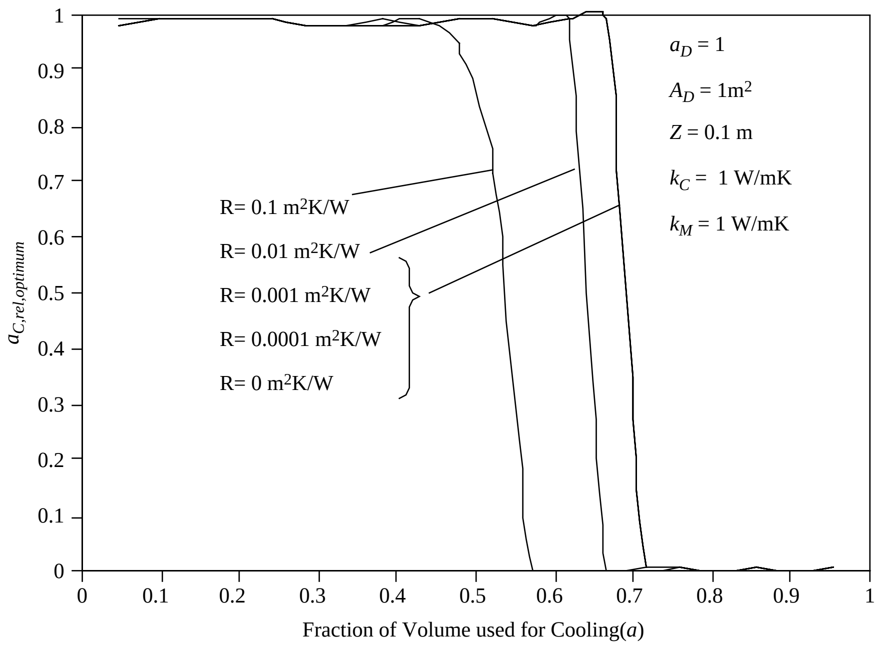

Figure 14.
Influence of thermal contact resistance on the optimum cooling shape for $A_D = 1\,\text{m}^2$ and $\mathscr{Z} = 0.1\,\text{m}$

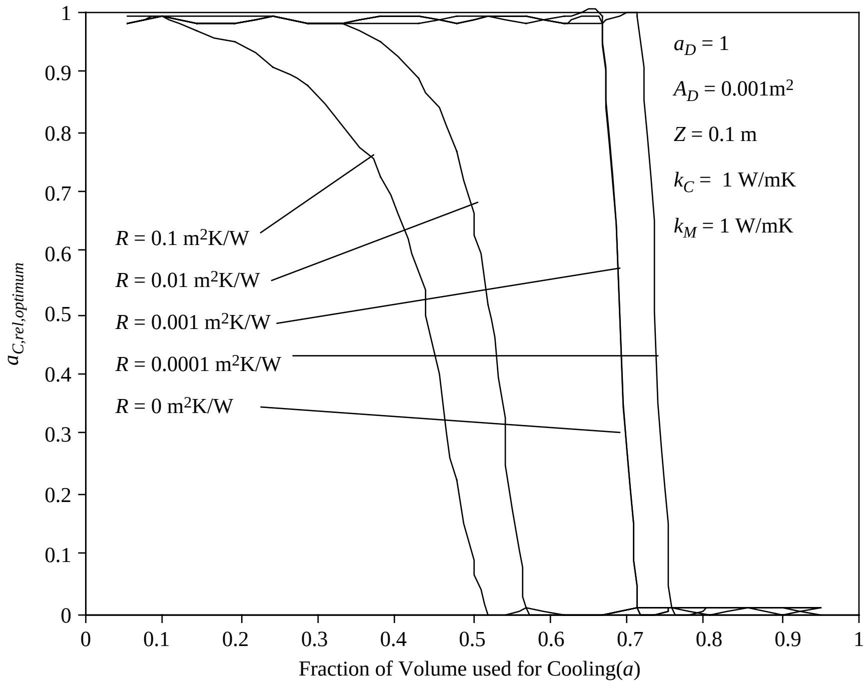

Figure 15.
Influence of thermal contact resistance on the optimum cooling shape for $A_D = 0.001\,\text{m}^2$ and $\mathscr{Z} = 0.1\,\text{m}$

Optimum $\mathrm{a}_{C,rel}$ *Results for* $\mathrm{a}_D = 2$

A domain with an aspect ratio of 2 represents a situation where the centre-to-centre distance between two adjacent cooling structures in one Cartesian coordinate direction is twice that in the other Cartesian direction. Figure 18 shows the behaviour of the optimum cooling shape for $a_D = 2$ at various R-values. It was found that, as before, the presence of thermal contact resistance strongly influences the optimum shape. It was also found that, unlike $a_D = 1$, the optimum cooling shape never has the same aspect ratio as the representative domain. It has a higher tendency to have a flat plate geometry as an optimum cooling shape.

Optimum $\mathrm{a}_{C,rel}$ *results for* $\mathrm{a}_D = 5$

When comparing $a_D = 2$ with $a_D = 5$, the latter has an even higher tendency toward optimum cooling shapes being continuous flat plates or layers. From Figure 19 it is clear that the influence of the thermal contact resistance is not as severe as before because the normalised optimum cooling shape aspect ratios have a much smaller spread. Similarly, the physical size of the cooling structure, A_D, has a smaller influence.

Optimum $\mathrm{a}_{C,rel}$ *results for* $\mathrm{a}_D = 10$

Similar trends were found to be true for higher representative domain aspect ratios, as shown in Figure 20. For the case of $a_D = 10$, it was observed that for almost the entire spectrum of domain fractions used by cooling, the optimum cross-sectional shape remained that of a flat plate.

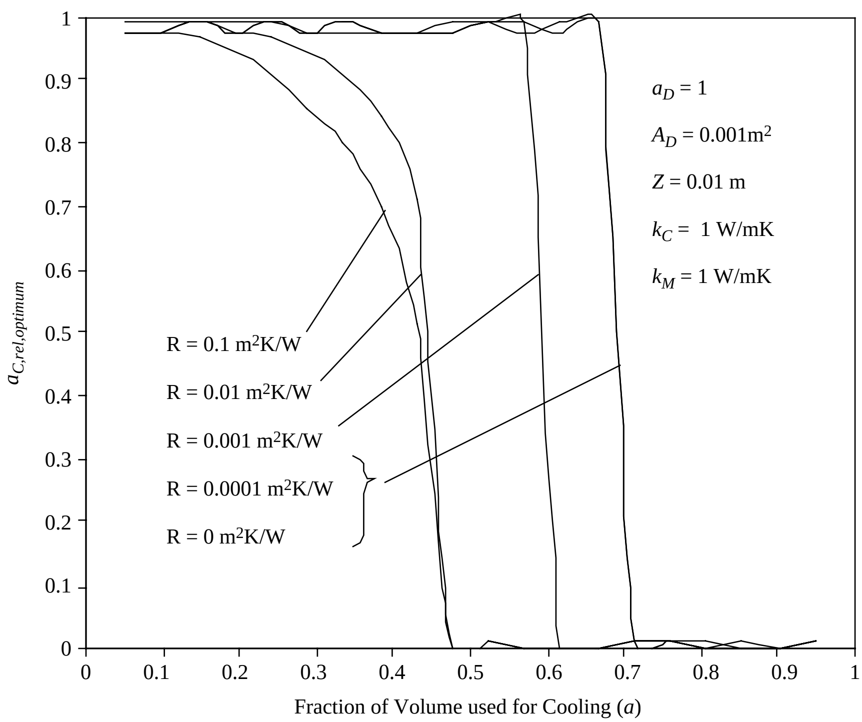

Figure 16.
Influence of thermal contact resistance on the optimum cooling shape for $A_D = 0.001\,\mathrm{m}^2$ and $\mathscr{Z} = 0.01\,\mathrm{m}$

Optimisation impact on thermal performance

It is furthermore important to determine when it is advantageous to optimise the cross-sectional aspect ratio of the extractor inserts in order to accommodate higher heat generation densities, while maintaining a certain maximum temperature within the representative domain. Thermal performance of a cooling insert scheme can be defined as the percentage by which heat generation density can be increased to such an extent that the structure is operated at the same peak temperature as it would have if no cooling inserts were present.

From optimisation runs it was found that, when no internal interface thermal resistance was present, the thermal performance increase obtained with a heat extractor scheme became less dependent on its cross-sectional shape as the ratio of A_D to $\mathscr{Z}^2$ decreased (Figure 21). At relatively larger ratios of A_D to $\mathscr{Z}^2$, additional thermal performance increases above that achieved by simply inserting cooling structures could be obtained by optimising the cooling shape. For low ratios of A_D to $\mathscr{Z}^2$, where the domain of a single insert becomes increasingly slender in the z direction, the advantage of optimising the cross-section in order to support higher heat generation levels diminishes. Subsequently, the thermal performance for narrow domains depends more on the fraction of the total volume occupied by the heat extraction system α than on the cross-sectional shape thereof.

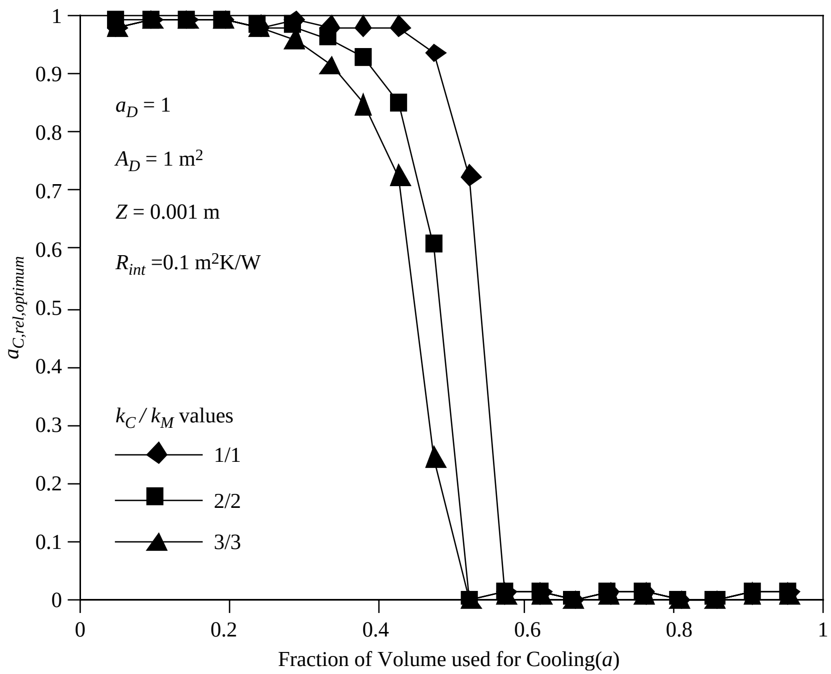

Figure 17.
Non-zero R for a constant ratio of thermal conductivity for $A_D = 1\,\text{m}^2$ and $\mathscr{Z} = 0.001\,\text{m}$

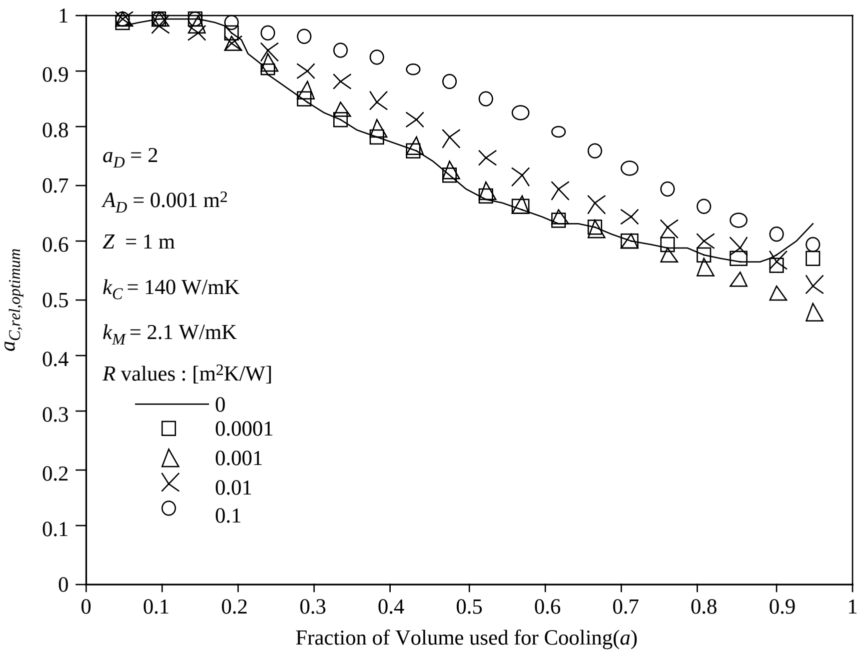

Figure 18.
Influence of R on the optimum cooling shape for $a_D = 2$

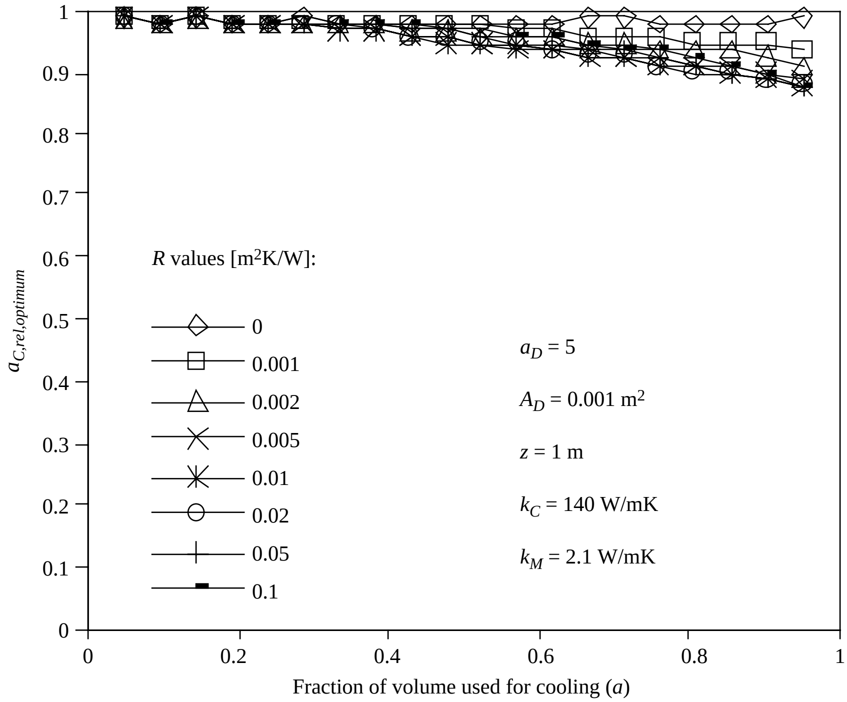

Figure 19.
Optimum cooling shape aspect ratios for $a_D = 5$ and various R values

It would therefore be sensible in such cases to use a cross-sectional geometry that is easier to manufacture or a geometry that would conform to other restrictions. Similar trends were obtained for beryllium oxide and synthetic diamond inserts. However, contrary to the trend shown in Figure 21, it was found that where thermal contact resistance is present, the influence of the cross-sectional shape remains significant for low A_D to $\mathscr{L}^2$ ratios. This phenomenon is recommended for further investigation.

Conclusions

Embedded conductive cooling inserts have the potential of decreasing operating temperatures within heat-generating mediums, such as those found in power electronics. In this investigation the thermal performance of rectangular cross-sectioned inserts that run parallel at uniformed offset spacing was analysed numerically. The objective was to find the optimum cooling insert aspect ratios that correspond to the lowest steady state peak temperatures for wide ranges of thermal, geometric and material property conditions.

The tendencies of optimised cooling shapes were described in terms of seven variables that have a significant impact on the optimum embedded cooling insert cross-sectional aspect ratio. These variables are the following: the centre-to-centre distance ratio between neighbouring inserts in the x- and y-directions; the physical size of the region between cooling inserts; the fraction of the total volume used for cooling; the z-directional distance through which heat needs to be conducted towards the

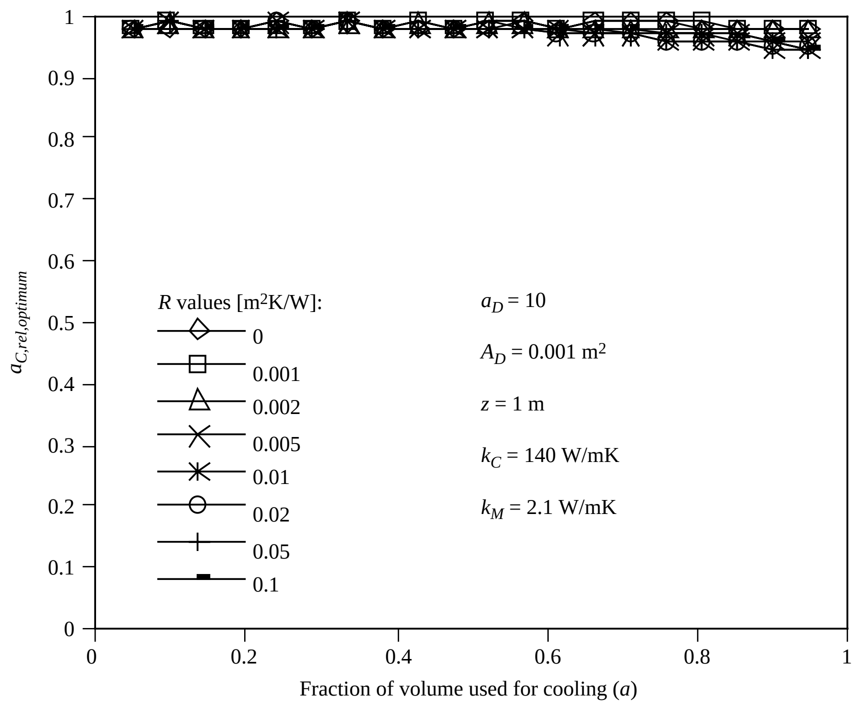

Figure 20.
Optimum cooling shape aspect ratios for $a_D = 10$ and various R values

surface of the heat-generating medium; the thermal interface resistance between the heat-generating medium and the cooling insert; and the thermal conductivities of the heat-generating and cooling mediums.

It was found that when no thermal interface contact resistance was present, the above list could be reduced to the centre-to-centre distance ratio between neighbouring inserts in the x- and y-directions, the fraction of the volume used for cooling, and the ratio between the thermal conductivities of the cooling insert material and the heat-generating medium. The study further showed that as the centre-to-centre distance ratio between neighbouring inserts in the x- and y-directions was increased, there was a greater tendency for the optimum cooling structure to be a continuous flat plate. The same was true for a decrease in the fraction of the volume used for cooling and the ratio between the thermal conductivities of the cooling insert material and the heat-generating medium. The influence of the physical size of the region between cooling inserts and the z-directional distance through which heat needs to be conducted towards the surface of the heat-generating medium is less obvious for small interface thermal resistance values.

The influence of thermal interface resistance itself is difficult to describe and falls beyond the scope of this investigation. However, it was found that thermal interface resistance causes the optimum cooling shape to deviate from being continuous layers at a smaller volume fraction than would have been the case if no thermal interface resistance had been present. In general, the same overall trends as for cases without thermal interface resistance were present.

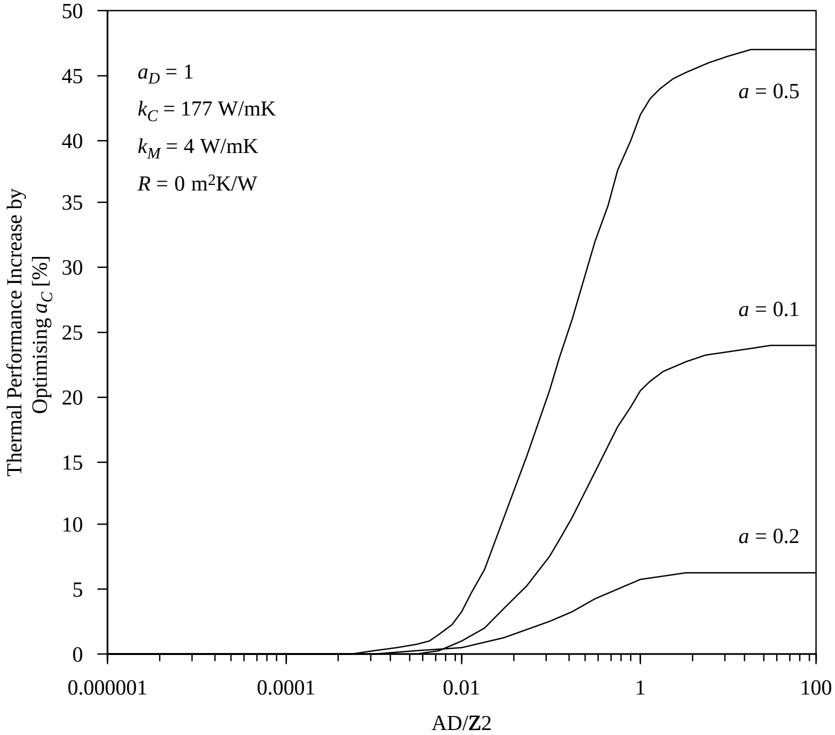

Figure 21.
Additional allowable increase in heat generation density after geometric optimisation

Finally, the study showed that as the region between cooling inserts becomes narrower in the *z*-direction, optimisation of the cooling insert aspect ratio has a smaller effect on the thermal performance increase of the cooling scheme. In such cases the ratio of volume use for cooling has a much greater effect on thermal performance. In cases where the region between cooling inserts is less slender and relatively shallow, geometric optimisation of the cooling shape is however still significant.

References

Barbosa, P., Lee, F.C., Van Wyk, J.D., Boroyevich, D., Scott, E., Thole, K., Odendaal, H., Liang, Z., Pang, Y., Sewell, E., Chen, J. and Yang, B. (2002), "An overview of IPEM-based modular implementation for distributed power systems", paper presented at Power Electronics Seminar, Centre for Power Electronics Systems (CPES), Virginia Tech, Blacksburg, VA, pp. 70-6.

Cerdán, J., Marín, J. and Martínez, A. (2002), "Polynomial preconditioners based on factorised sparse approximate inverses", *Applied Mathematics and Computation*, Vol. 133, pp. 171-86.

Ferreira, J.A. and Gerber, M. (2002), "Three-dimensional integration based on power module technology", *Proceedings of the 2nd International Conference on Integrated Power Systems (CIPS)*, pp. 35-41.

Fröberg, C-E. (1985), *Numerical Mathematics: Theory Band Computer Applications*, The Benjamin/Cummings Publishing Company, Inc., New York, NY, pp. 149-53.

Gajewsk, R.R. and Lompies, P. (1999), "Object-oriented approach to the reduction of matrix bandwidth, profile and wavefront", *Advances in Engineering Software*, Vol. 30, pp. 783-8.

Lee, F.C., Van Wyk, J.D., Boroyevich, D., Jahns, T., Chow, T. and Barbosa, P. (2002), "Modularisation and integration as a future approach to power electronic systems", *Proceedings of the 2nd International Conference on Integrated Power Systems (CIPS)*, pp. 9-18.

Liu, X. and Lu, G.-Q. (2000), "Power electronics packaging and miniature using chip-scale packaged power devices", paper presented at The Third International Power Electronics and Motion Control Conference Proceedings, PIEMC 2000,Vol. 1, pp. 246-51.

Patankar, S.V. (1980), *Numerical Heat Transfer and Fluid Flow*, Hemisphere, Washington, DC.

Strydom, J.T. and Van Wyk, J.D. (2002), "Improved loss determination for planar integrated power passive modules", paper presented at Power Electronics Seminar, Centre for Power Electronics Systems (CPES), Virginia Tech, Blacksburg, VA, pp. 415-21.

Van Wyk, J.D., Strydom, J.T., Zhao, L. and Chen, R. (2002), "Review of the development of high density integrated technology for electromagnetic power passives", *Proceedings of the 2nd International Conference on Integrated Power Systems (CIPS)*, pp. 25-34.

Wolfgang, E., Seliger, N., Lugert, G. and Riepl, T. (2002), "High-temperature power electronics: challenges and opportunities", *Proceedings of the 2nd International Conference on Integrated Power Systems (CIPS)*, pp. 43-51.

Yang, L., Lee, F.C. and Odendaal, W.G. (2003), "Measurement-based characterisation method for integrated power electronics modules", paper presented at Eighteenth Annual IEEE Applied Power Electronics Conference and Exposition, APEC '03,Vol. 1, pp. 490-6.

About the authors

Jaco Dirker obtained his BE (*cum laude*) in 2000 in Mechanical Engineering, BSc (*cum laude*) in 2002 in Mathematics and Applied Mathematics, ME (*cum laude*) in 2002 in Mechanical Engineering, and PhD in 2004 also in Mechanical Engineering from the Rand Afrikaans University in Johannesburg, South Africa. In 2004 he joined the Department of Mechanical and Aeronautical Engineering at the University of Pretoria, South Africa as a Lecturer. His research interests include, conductive and convective heat transfer, and cooling of electronics. Jaco Dirker is the corresponding author and he can be contacted at: jaco.dirker@up.ac.za

Arnaud G. Malan received his BE and ME degrees in Mechanical Engineering from the University of Pretoria, South Africa, in 1994 and 1996, respectively, and a PhD degree from the University of Wales, Swansea in the UK in 2003. The field of research for the latter was computational fluid dynamics. Prior to embarking on PhD studies, he worked in industry from 1995 to 1999, starting in the final year of his Master's studies. During the first year he acted as a consulting engineering designing air-conditioning systems, followed by finite element-based structural analysis and design work at BKS Advantech (Pty) Ltd He has been a Senior Lecturer at the Department of Mechanical and Aeronautical Engineering of the University of Pretoria since 2003. In 2006 he was promoted to Associate Professor in the same department. Malan has been the recipient of a number of prestigious scholarships and awards. He was granted a Commonwealth Scholarship for Research in Mechanical Engineering leading to the degree of PhD from the Association of Commonwealth Universities in 1999. In 2003 he received the *Best PhD Thesis for year 2002* award from the Association of Computational Mechanics in Engineering (UK), and was bestowed with a Young Researcher Fellowship for Exemplary Research in Computational Mechanics at the Second Massachusetts Institute of Technology

Conference on Computational Fluid and Solid Mechanics in the same year. Malan is registered as a professional engineering at the Engineering Council of South Africa and is an executive committee member of the South African Association for Theoretical and Applied Mechanics.

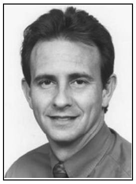

Josua P. Meyer obtained his BE (*cum laude*) 1984, ME (*cum laude*) 1986, and his PhD (1988) all in Mechanical Engineering from the University of Pretoria. He is registered as a Professional Engineer and he completed his military service at the Faculty of Military Science, University of Stellenbosch where he lectured aerodynamics for pilots in the South African Air Force. After his military service (1988-1989), he accepted a position as Associate Professor in the Department of Mechanical Engineering at the Potchefstroom University in 1990. He was Acting Head and Professor in Mechanical Engineering before accepting a position as Professor in the Department of Mechanical and Manufacturing Engineering at the Rand Afrikaans University in 1994. He was the Chairman of Mechanical Engineering from 1999 until the end of June 2002 after which he was appointed as Professor and Head of the Department of Mechanical and Aeronautical Engineering of the University of Pretoria from 1 July 2002. He is a Chairman of the School of Engineering since 1 January 2004. The School consists of eight departments totalling more than 4,000 students. He specializes in heat transfer, fluid mechanics and thermodynamic aspects of heating, ventilation and air-conditioning. He is the author and co-author of more than 200 articles, conference papers and patents and has received various prestigious awards for his research. He is also a fellow or member of various professional institutes and societies (i.e. South African Institute for Mechanical Engineers, South African Institute for Refrigeration and Air Conditioning, American Society for Mechanical Engineers, American Society for Air-Conditioning, Refrigeration and Air-Conditioning) and is regularly invited to be a keynote speaker at local and international conferences. He has also received various teaching awards as Lecturer of the Year (at the Potchefstroom University and Rand Afrikaans University) as well as an Exceptional Academic Achievers award by the University of Pretoria. He is also a rated researcher by the NRF.